Hydrogen diffusion in tungsten: A molecular dynamics study

Yi-Nan Liu [a], Tiefeng Wu [b], Yi Yu [a], Xiao-Chun Li [c], Xiaolin Shu [a,*], Guang-Hong Lu [a]

[a] School of Physics & Nuclear Energy Engineering, Beihang University, Beijing 100191, China
[b] Shanghai Aircraft Design and Research Institute, Shanghai 201210, China
[c] Institute of Plasma Physics, Chinese Academy of Sciences, Hefei, Anhui 230031, China

ARTICLE INFO

ABSTRACT

The diffusion behavior of hydrogen (H) in tungsten (W) has been studied by molecular dynamics simulations. The diffusivities from 200 K to 3000 K are calculated and the diffusion equation is fitted to $D = 5.13 \times 10^{-8} \exp(-0.21\ \text{eV}/kT)\ \text{m}^2/s$. The diffusion equations in different temperature ranges of 200–500 K, 500–2400 K and 2400–3000 K are also given separately and the results imply different H diffusion modes in different temperature ranges, which is proved by analyzing equilibrium H positions at low and high temperatures. The H atom jumps between different tetrahedral interstitial sites (TISs) at lower temperatures, but the transition to octahedral interstitial sites (OISs) is also observed at high temperatures. Moreover, with a vacancy present in the W system, vacancy trapping of H is observed, and it is shown that the vacancy trapping reduces with the increasing temperature. The H binding energy to monovacancy is obtained using three different methods including NEB and fitting both H diffusivity and time for H to detrap from the vacancy, which provides more information of the H behaviors with the existence of defects.

© 2014 Elsevier B.V. All rights reserved.

1. Introduction

Tungsten (W) is now considered as one important candidate for the plasma facing materials (PFMs) in fusion devices because of its excellent material properties such as high melting temperature, high thermal diffusivity, and low sputtering yield. However, recent experiments demonstrated that hydrogen (H) blisters can be formed when W is exposed to the high flux plasma irradiation with quite low incident energies [1,2], and the bursting of blisters would both shorten the material lifetime and reduce the plasma performance. Therefore, this blistering problem induced by H retention is now one of the most challenging issues for the PFMs design. To understand the underlying mechanism, the diffusion behavior of H in W requires extensive study. As the incident energy of H isotopes in ITER is less than 100 eV, the implanted H atoms are basically within dozens of nanometers of the surface according to the theoretical calculations [3]. However, unlike the Helium bubbles appearing within ~100 Å at the surface [4], the depth distribution of H measured in experiments and the bubble formation are in the scale of microns [5–8], suggesting that H diffusion plays a significant role.

As one of fundamental factors affecting the retention and blistering, the diffusivities of H in different temperature regions and different kinds of W samples are investigated and summarized

[9,10]. Among the numerous experimental investigations, the diffusivity of H in W was measured by Frauenfelder et al. [11] for a wide temperature range of 1100–2400 K and the diffusion equation was given as $D = 4.1 \times 10^{-7} \exp(-0.39\ \text{eV}/kT)\ \text{m}^2/s$. Theoretical studies were also carried out to investigate H diffusion. First-principles calculations were performed by Liu et al. [12] and the diffusion barrier between adjacent tetrahedral interstitial sites (TISs) was given as 0.20 eV using the drag method. Meanwhile, the nudged elastic band (NEB) method was used by Heinola et al. [13] yielding a diffusion barrier in W of 0.21 eV for H by first-principles simulations as well. They also obtained the diffusion prefactor as $5.2 \times 10^{-8}\ \text{m}^2/s$ using harmonic transition state theory throughout the range of 1100–2400 K. As for molecular dynamics (MD) simulations, the diffusivity of H in bulk W calculated by Juslin et al. [14] with an analytical bond-order potential (BOP-Juslin) was: $D = 3.18 \times 10^{-8} \exp(-0.34\ \text{eV}/kT)\ \text{m}^2/s$. However, the cut-off distance of the W–H interaction is too short in this potential, which is 2.35 Å and less than the first nearest neighbor distance of body-centered cubic (bcc) W. This implies that a sub-situational H atom will not interact with its first nearest neighbor W atom [15]. To describe the interactions of H atoms with W with the presence of defects, a modified bond-order potential for W–H systems is constructed by Li et al. [16] and used here to study the H diffusion behaviors in W with and without vacancy.

In this work, we investigate H diffusion in W by MD simulations. The diffusivities of H in W at different temperatures are

---

obtained by calculating the mean square displacement of the H atom as a function of time, and the Arrhenius' diffusion equation is fitted for the whole temperature range. The H diffusion mechanism is also studied by fitting the diffusion equations in different temperature zones and analyzing the diffusing paths. Furthermore, the trapping effect of monovacancy on H diffusion at different temperatures is also investigated and three different methods are applied to obtain the energy barrier for H atom to detrap from the vacancy.

2. Methodology

The MD code LAMMPS [17] is used to study the diffusion behavior of H in W. The simulation box consists of 10 unit cells of W atoms with bcc crystal structure, and contains a single H atom located at a TIS position initially. Periodic boundary conditions are applied in all three directions and the temperature of the system is scaled at certain target temperatures between 200 K and 3000 K. The diffusion time of H in W is 5 ns at each temperature.

For data analysis, the diffusivity of H in W is calculated using the Einstein equation from random walk theory shown as

$$D = \frac{\langle [r(t) - r(0)]^2 \rangle}{6t} \tag{1}$$

where D is the diffusivity, t is the diffusion time, and r is the position of the H atom. The mean square displacement (MSD) value for H is calculated by

$$\left\langle [r(t) - r(0)]^2 \right\rangle = \frac{1}{n_i} \sum_i [r_i(t) - r_i(0)]^2 \tag{2}$$

In addition, the temperature dependence of the diffusivity can be expressed as the Arrhenius' equation:

$$D = D_0 \exp\left[-\frac{E_a}{k_B T}\right] \tag{3}$$

where D_0 is the prefactor of diffusion, k_B is the Boltzmann constant and E_a is the activation energy for diffusion. This equation can be written as the following form:

$$\ln D = \ln D_0 - E_a/k_B T. \tag{4}$$

It is shown from the above equation that the logarithm of diffusivity $\ln D$ is linear with the reciprocal of temperature. Thus in this work, we use these two variables to fit the logarithm form of Arrhenius' equation.

3. Results and discussion

3.1. H diffusion in bulk W

The MSD data of an H atom in W at a given temperature are calculated and fitted as a function of the diffusion time, as shown in Fig. 1. The 29 fitting lines are shown, each one representing a MSD/6-t relation of a single H atom in bulk W under a certain temperature from 200 K to 3000 K. Then according to Eq. (1), the diffusivity of H in W under a given temperature is given by the slope of each curve. The results of diffusivities yielded by the linear fitting are listed in Table 1.

To obtain a general description of the diffusion behavior of single H atom in W, we use the data from Table 1 and Eq. (4) to fit the diffusion equation over the entire simulation range. We set the reciprocal of temperature ($10^4/T$) as x axis, and the logarithm of diffusivity ($\ln D$) as y. A linear least square fit for the diffusion prefactor and activation energy gives values for these as 5.13×10^{-8} m^2/s and 0.21 eV, respectively, as shown in Fig. 2. The comparison of the results from our simulation and other
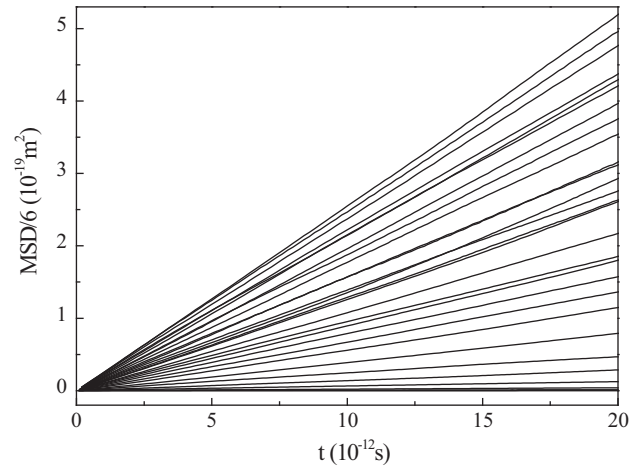

Fig. 1. The mean square displacement information (MSD/6) of a single H atom in W at the temperature from 200 K to 3000 K.

Table 1
The diffusivity of a single H atom in bulk W at a given temperature from 200 K to 3000 K.

T (K)	D (m^2/s)	T (K)	D (m^2/s)	T (K)	D (m^2/s)
200	7.033×10^{-13}	1200	7.873×10^{-09}	2200	1.749×10^{-08}
300	1.439×10^{-11}	1300	9.132×10^{-09}	2300	1.929×10^{-08}
400	7.942×10^{-11}	1400	9.523×10^{-09}	2400	1.975×10^{-08}
500	2.438×10^{-10}	1500	1.107×10^{-08}	2500	2.034×10^{-08}
600	6.904×10^{-10}	1600	1.269×10^{-08}	2600	2.200×10^{-08}
700	1.470×10^{-09}	1700	1.308×10^{-08}	2700	2.171×10^{-08}
800	2.520×10^{-09}	1800	1.456×10^{-08}	2800	2.410×10^{-08}
900	3.924×10^{-09}	1900	1.416×10^{-08}	2900	2.612×10^{-08}
1000	5.484×10^{-09}	2000	1.629×10^{-08}	3000	2.593×10^{-08}
1100	6.715×10^{-09}	2100	1.666×10^{-08}		

$D_0 = 5.13 \times 10^{-8} \ m^2/s$
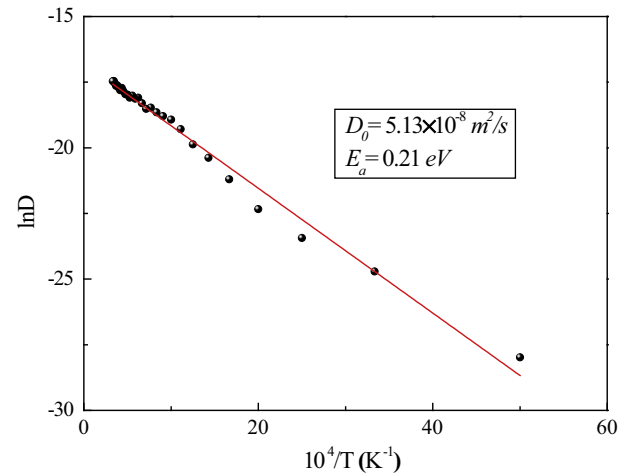$E_a = 0.21 \ eV$

Fig. 2. The Arrhenius' fit (red line) for H diffusion in W from 200 K to 3000 K. (For interpretation of the references to color in this figure legend, the reader is referred to the web version of this article.)

Table 2
The prefactors and activation energies for H diffusion in W from the present work and other methods.

	Present work	BOP-Juslin [14]	DFT [12,13]	Experiment [11]
D_0 (m^2/s)	5.13×10^{-8}	3.1×10^{-8}	5.2×10^{-8} [13]	4.1×10^{-7}
E_a (eV)	0.21	0.34	0.20 [12], 0.21 [13]	0.39

methods are listed in Table 2. Both the activation energy and the prefactor obtained in present work are in good agreement with the DFT results.

Compared with the experimental results of 0.39 eV [11], the activation energies from both our fitting result 0.21 eV and DFT calculations 0.20 eV [12] are found to be smaller. For DFT calculations, it is known that the most stable interstitial site for an H atom in W is the TIS position and the octahedral interstitial site (OIS) is a sub-stable position [12,16], thus there are two possible migration paths for H diffusion, which are TIS–TIS and TIS–OIS–TIS. Previously it is believed that the H atom diffuses along the TIS–TIS path, which is energetically preferred with activation energy of 0.20 eV [12]. However, we noticed that the energy barrier of TIS–OIS–TIS path given by DFT calculation is 0.38 eV [12], which is quite close to the experiment result. Similarly, the energy barriers along the TIS–TIS and TIS–OIS–TIS paths are given as 0.23 eV and 0.43 eV for our potential in MD simulation, respectively [16]. Thus the comparison of experimental value and simulation results has led us to consider the possibility of having a different diffusion path at a high temperature. It is known that in order to leave out the trapping effect, the experiment is carried out at a high temperature regime from 1100 K to 2400 K [11], so a higher energy diffusion path could also become possible at such high temperatures.

We then divide the temperature regime into 3 zones, i.e., zone A (200–500 K), zone B (500–2400 K), and zone C (2400–3000 K), according to the linear fit shown in Fig. 2. The fitting results are listed in Table 3. The prefactors and activation energies for zone A, B and C are also shown.

It is clear from Table 3 that both D_0 and E_a increase with temperature. The increase of activation energy with temperature indicates the involvement of migration paths with higher migration energies. Moreover, the activation energies for the lower and higher temperature ranges approximately coincide with the energy barriers of the paths TIS–TIS and TIS–OIS–TIS, respectively. Thus it is assumed that besides the TIS–TIS path, H atoms may diffuse along TIS–OIS–TIS path as well when the temperature increases.

In order to look into the details of H diffusion in different temperature zones, we have analyzed the H positions during the migration at 400 K and 2600 K and plotted part of the results in Fig. 3. At the lower temperature of 400 K, H prefers to vibrate around the TIS, and move to the nearest neighboring TIS. The diffusion path is mainly TIS–TIS as shown in Fig. 3(a). However, as the temperature increases, H becomes more active, and it may migrate from one TIS to another TIS by passing through an OIS as shown in Fig. 3(b) at 2600 K. The migrating path of H in W is a mixture of the TIS–TIS and TIS–OIS–TIS paths at a high temperature.

In short, we believe that the H diffusion mechanism changes with different temperatures ranges. The H atom mainly diffuses along the TIS–TIS path at low temperature, but as the temperature increases, the probability of diffusion along the TIS–OIS–TIS path also increases, and in that case, TIS–TIS is not the only choice for H diffusion. This could be the reason for the observation of the increasing activation energy with the increasing temperature.

3.2. H diffusion in W with vacancy

To study the vacancy trapping on H diffusion in W, we create a vacancy (V) in the perfect bulk W system with 2000 atoms and the H atom is initially put at the near OIS position in the vacancy, which has been shown to be the most stable structure for single H + V [18]. The vacancy is created by removing one W atom in the center of the system, which means that the vacancy concentration is 5×10^{-4}. All the other conditions remain the same as in the perfect bulk simulations and each run also lasts 5 ns.

According to the results found in this study, when the temperature is below 1900 K, the H atom is trapped by the vacancy, thus it is difficult to achieve the diffusivity within the MD time scale. The results with temperature above 1900 K are shown in Fig. 4. The relation between the logarithm of diffusivity and the reciprocal of temperature with the presence of the monovacancy (semi-circle line) is given together with the results of perfect lattice (dotted line) so as to study the influence of vacancy on H diffusion. The trapping influence of a vacancy on H is clearly demonstrated in Fig. 4. And it is obvious that the trapping effect decreases with increasing temperature, which could be seen from the narrowing of the gap between curves with and without the vacancy in Fig. 4. It is also clear from the curve that even if the H atom could detrap from the vacancy and migrate, the relationship between the

Table 3
The fitting results of Arrhenius' equations for a single H atom in bulk W in different temperature zones.

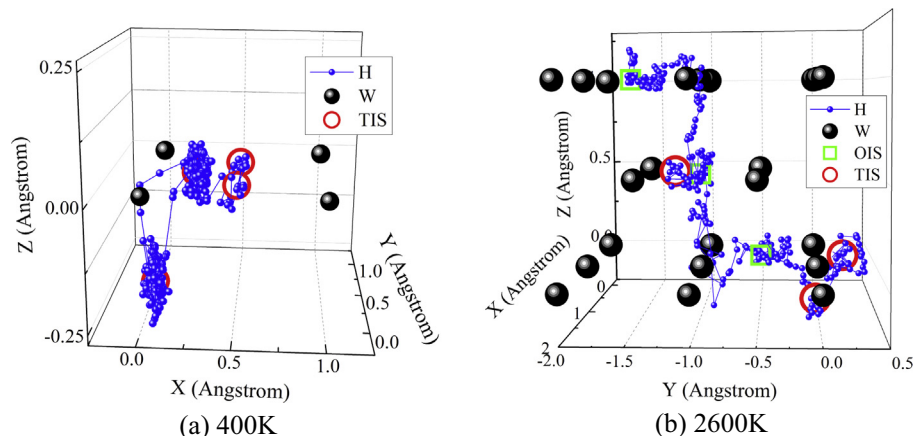| Zone	Diffusion Equation	D_0 (m^2/s)	E_a (eV)
A (200–500 K)	$D = 7.88 \times 10^{-9} \exp(-0.16\ eV/kT)$ m^2/s	7.88×10^{-9}	0.16
B (500–2400 K)	$D = 7.01 \times 10^{-8} \exp(-0.24\ eV/kT)$ m^2/s	7.01×10^{-8}	0.24
C (2400–3000 K)	$D = 1.06 \times 10^{-7} \exp(-0.36\ eV/kT)$ m^2/s	1.06×10^{-7}	0.36

(a) 400K   (b) 2600K

Fig. 3. The H positions during diffusion in W at 400 K and 2600 K, shown in (a) and (b), respectively. The H atom jumps between TISs at 400 K, as in (a). However, it also goes through the OISs at 2600 K, shown in (b).
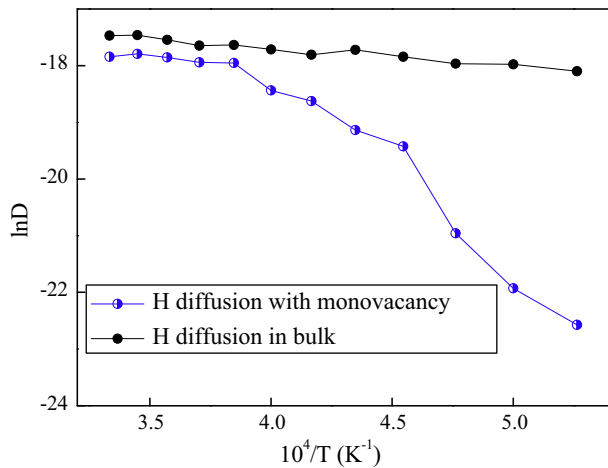
Fig. 4. The comparison of H diffusion behavior with and without a vacancy between 1900 K and 3000 K. The curve with black dots shows the diffusion behavior in perfect bulk W and the blue semi-circle line gives the diffusion behavior in W with the monovacancy.

logarithm of diffusivity and the reciprocal of temperature could not be described linearly. At such high temperatures, besides the H dissociation from the vacancy and diffusion, other processes such as the recombination of H and vacancy, and the vacancy diffusion are also observed, so it is hard to describe all these processes by the Arrhenius' relationship.

In order to get more details about the H-vacancy binding, we conduct an NEB simulation to obtain the energy required for an H atom to dissociate from the monovacancy, which is shown in Fig. 5. An energy barrier of 1.90 eV is required for the H atom to overcome the binding with the monovacancy and a total energy about 2.35 eV is needed for H to diffuse away from the vacancy. It is also obvious that far away from the vacancy, the energy difference of 0.23 eV is exactly the same as the lowest energy barrier between adjacent TISs in the bulk for our potential [16].

As a comparison, we still linearly fit the result curve with vacancy in Fig. 4 and got the equation $D = 2.03 \times 10^{-4} \exp(-2.22 \text{ eV}/kT)$ m^2/s. An energy barrier of 2.22 eV is yielded. Taken into consideration of the H diffusion barrier of 0.21 eV, the binding energy would be 2.01 eV.

To further understand the process of H dissociation and the following migration, we have analyzed the movements of both H atom and the vacancy. A Wigner–Seitz analysis [19,20] is applied
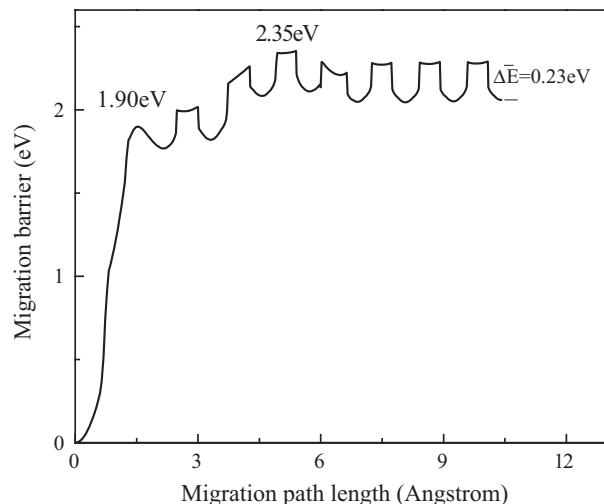

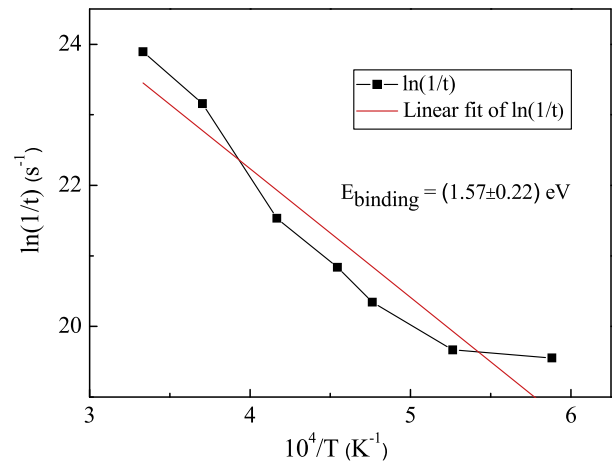**Fig. 5.** The migration barrier for an H atom to detrap from a single vacancy using NEB simulation.

Fig. 6. The Arrhenius' fit for the H detrapping time from the monovacancy. The binding energy of (1.57 ± 0.22) eV is obtained from the slope of the linear fitting.

Table 4
The binding energy and trapping energy for single H atom in monovacancy using different methods (eV).

	Present work			DFT [21]
	NEB	Fit lnD	Fit ln(1/t)	
Binding energy	1.90	2.01	1.57	1.43
Trapping energy	2.35	2.22	1.78	1.60

to get the vacancy information during the simulation. Thus we could obtain the time for an H atom to jump out of the vacancy and start diffusing in the whole simulation system at a certain temperature. Since the reciprocal of this time represents the H detrapping ratio, we also fit the relationship between the reciprocal of detrapping time with the reciprocal of temperature, which should also follow the Arrhenius' equation, as shown in Fig. 6. As a result, an energy barrier of (1.57 ± 0.22) eV is yielded and represents the binding between H atom and the monovacancy. This value is slightly lower than the results of NEB method and the fitting of diffusivity with monovacancy, but quite close to the DFT calculation [21]. Results from the three different methods we have used in this work are listed in Table 4 and compared with the DFT calculation.

4. Summary

We have carried out the MD simulations to investigate the hydrogen diffusion properties in tungsten using a modified analytical bond-order potential which is especially suitable to describe the W–H system with defects. The mean square displacements of an H atom are calculated to obtain H diffusivity in a wide temperature range of 200–3000 K. The Arrhenius' equation is achieved by fitting the whole region as $D = 5.13 \times 10^{-8} \exp(-0.21 \text{ eV}/kT)$ m^2/s. Moreover, the diffusion process is also studied by dividing the temperature region into different zones of 200–500 K, 500–2400 K, and 2400–3000 K and separate fitting results indicate the possibility of different diffusion paths in different temperature regions. The H atom diffuses along the TIS–TIS (tetrahedral interstitial site) path when the temperature is low. However, with the temperature increasing, the possibility for the H atom to jump to the sub-stable octahedral interstitial site (OIS) also rises and diffusion along TIS–OIS–TIS could also occur. In a higher temperature region, the diffusion of H atom is a combination of both. This is proved by analyzing H positions during the diffusion process at 400 K and 2600 K.

The vacancy trapping of H is quite obvious since the H atom is captured by the vacancy and the MSD approaches zero when the temperature is below 1900 K, and from the comparison of the

results with and without the vacancy, it is shown that vacancy trapping is reduced significantly with increasing temperature. Moreover, the H binding energy to monovacancy is obtained using three different methods including NEB and fitting both H diffusivity and time for H to detrap from the vacancy, which provides more information of the H behaviors with the existence of defects.

Acknowledgments

References

[1] W.M. Shu, E. Wakai, T. Yamanishi, Nucl. Fusion 47 (2007) 201–209.
[2] G.N. Luo, W.M. Shu, M. Nishi, J. Nucl. Mater. 347 (2005) 111–117.
[3] Z. Yang, Q. Xu, R. Hong, Q. Li, G.-N. Luo, Fusion Eng. Des. 85 (2010) 1517–1520.
[4] R.J.K. Nicholson, J.M. Walls, J. Nucl. Mater. 76–77 (1978) 251–252.
[5] V.K. Alimov, J. Roth, Phys. Scr. T128 (2007) 6–13.
[6] G.M. Wright, M. Mayer, K. Ertl, G. de Saint-Aubin, J. Rapp, Nucl. Fusion 50 (2010) 075006.
[7] W.M. Shu, G.N. Luo, T. Yamanishi, J. Nucl. Mater. 367–370 (2007) 1463–1467.
[8] W.M. Shu, A. Kawasuso, T. Yamanishi, J. Nucl. Mater. 386–388 (2009) 356–359.
[9] A.C. Rion, J.V. Thomas, Phys. Scr. 2001 (2001) 9.
[10] R.A. Causey, J. Nucl. Mater. 300 (2002) 91–117.
[11] R. Frauenfelder, J. Vac. Sci. Technol. 6 (1969) 388–397.
[12] Y.-L. Liu, Y. Zhang, G.N. Luo, G.-H. Lu, J. Nucl. Mater. 390–391 (2009) 1032–1034.
[13] K. Heinola, T. Ahlgren, J. Appl. Phys. 107 (2010) 113531.
[14] N. Juslin, P. Erhart, P. Träskelin, J. Nord, K.O.E. Henriksson, K. Nordlund, E. Salonen, K. Albe, J. Appl. Phys. 98 (2005) 123520.
[15] X.-C. Li, F. Gao, G.-H. Lu, Nucl. Instrum. Methods Phys. Res., Sect. B 267 (2009) 3197–3199.
[16] X.-C. Li, X. Shu, Y.-N. Liu, F. Gao, G.-H. Lu, J. Nucl. Mater. 408 (2011) 12–17.
[17] S. Plimpton, J. Comput. Phys. 117 (1995) 1–19.
[18] Y.-L. Liu, Y. Zhang, H.-B. Zhou, G.-H. Lu, F. Liu, G.N. Luo, Phys. Rev. B 79 (2009) 172103.
[19] N. D. M Neil, W. Ashcroft, Solid State Physics, Saunders College, Orlando, 1976.
[20] N. Juslin, V. Jansson, K. Nordlund, Phil. Mag. 90 (2010) 3581.
[21] K. Heinola, T. Ahlgren, K. Nordlund, J. Keinonen, Phys. Rev. B 82 (2010) 094102.